

Flood event attribution and damage estimation using national-scale grid-based modelling: Winter 2013/14

| | |
|-------------------------------|--|
| Journal: | <i>International Journal of Climatology</i> |
| Manuscript ID | JOC-17-0760 |
| Wiley - Manuscript type: | Research Article |
| Date Submitted by the Author: | 05-Oct-2017 |
| Complete List of Authors: | Kay, Alison; Centre for Ecology and Hydrology, Water and Pollution Science Booth, Naomi; JBA Risk Management Limited, JBA Risk Lamb, Rob; JBA Trust, JBA Trust Raven, Emma; JBA Risk Management Limited, JBA Risk Schaller, Nathalie; CICERO Centre for International Climate and Environmental Research, CICERO Centre for International Climate and Environmental Research Sparrow, Sarah; University of Oxford, Oxford e-Research Centre |
| Keywords: | Flooding, Climate change, inundation, property damage |
| Country Keywords: | United Kingdom Of Great Britain And Northern Ireland |
| | |

SCHOLARONE™
Manuscripts

Only

1 **Flood event attribution and damage estimation using national-scale grid-based**
2 **modelling: Winter 2013/14.**

3

4 Short title: Winter 2013/14 flood attribution and damage estimation

5

6 Kay A.L.¹, Booth N.², Lamb R.^{3,4}, Raven E.², Schaller N.^{5,6}, Sparrow S.⁷

7 ¹ Centre for Ecology & Hydrology, Maclean Building, Wallingford, OX10 8BB, UK

8 ² JBA Risk Management Limited, South Barn, Broughton Hall, Skipton, BD23 3AE,
9 UK

10 ³ JBA Trust, South Barn, Broughton Hall, Skipton, BD23 3AE, UK

11 ⁴ Lancaster Environment Centre, Lancaster University, Lancaster, LA1 4YQ, UK

12 ⁵ CICERO Centre for International Climate and Environmental Research, Oslo, Norway

13 ⁶ Environmental Change Institute, University of Oxford, Oxford, OX1 3QY, UK

14 ⁷ Oxford e-Research Centre, University of Oxford, Oxford, OX1 3QG, UK

15

16 **Abstract**

17 A sequence of major flood events in Britain over the last two decades has prompted
18 questions about the influence of anthropogenic greenhouse gas emissions on flood risk.

19 Such questions are difficult to answer definitively, as a range of other factors are
20 involved, but modelling techniques allow an assessment of how much the chance of
21 occurrence of an event could have been altered by emissions. Here, the floods of Winter
22 2013/14 in Britain are assessed by combining ensembles of climate model data with a
23 national-scale hydrological model and, for one severely-impacted river basin (the

24 Thames), a detailed analysis of flood inundation and the increased number of residential
25 properties placed at risk. One climate model ensemble represents the range of possible
26 weather under the current climate, while 11 alternative ensembles represent the weather
27 as it could have been had past emissions not occurred. The results show that emissions
28 are likely to have increased the chance of occurrence of these floods across much of the
29 country, with a stronger influence on longer duration peaks (~10 days or more) than for
30 shorter durations (consistent with observations). The influence on flows and property
31 flooding varies spatially, due to both spatial variation in the influence on precipitation
32 and variation in physical properties that affect the transformation of precipitation to
33 river flow and flood impacts, including flood defences. This complexity highlights the
34 importance of using hydrological modelling to attribute hydrological impacts from
35 meteorological changes. Changes in snow occurrence in a warming climate are also
36 shown to be important, with effects varying spatially.

37

38 **Keywords**

39 Flooding, climate change, inundation, property damage

40

41 **1 Introduction**

42 It is now widely accepted that climate change will have significant impacts on the
43 hydrological cycle, globally and regionally, and there are increasing signs of
44 hydrological changes having already occurred, rather than just being a concern for the
45 future (Jiménez Cisneros et al. 2014, Blöschl et al. 2017). Detection and attribution of
46 observed hydrological changes to anthropogenic emissions is difficult however, due to

47 the influence of a range of other factors (both anthropogenic and natural) and because
48 available records are often relatively short (Hannaford 2015), making statistical tests
49 prone to uncertainty.

50 In the UK, there is evidence of observed changes in precipitation, evaporation and river
51 flows, although with varying levels of confidence and little evidence to link them to
52 anthropogenic climate change (Watts et al. 2015). Although there has been little change
53 in annual mean precipitation for England and Wales (since records began in 1766), there
54 have been winter increases and summer decreases, and more recent changes in heavy
55 rainfall (Jenkins et al. 2008). There have also been increases in evaporation (Kay et al.
56 2013) and decreases in snow (Kay 2016). Each of these is likely to have affected river
57 flows; analyses suggest increases in annual and winter runoff across Britain but
58 decreases in summer runoff for England (1961-2011), along with increases in high flow
59 magnitude and duration to the north and west of Britain, although the latter are not
60 always coincident with increases in peak flows like annual maxima (Hannaford 2015).

61 Floods are one of the most damaging natural hazards, threatening lives and livelihoods
62 worldwide. Floods present the most serious natural hazard in the UK, with over 5
63 million properties considered at risk of flooding from one or more sources (rivers,
64 surface water, coastal) (Thorne 2014). A sequence of major floods has occurred in
65 Britain over the last two decades (Hannaford 2015); Easter 1998 (the Midlands),
66 Autumn 2000 (much of England and Wales), Summer 2007 (central and northern
67 England), November 2009 (north-west Britain), Summer/Autumn 2012 (much of
68 Britain) and, more recently, Winter 2013/14 (southern England; Huntingford et al.
69 2014) and December 2015 (northern Britain; Barker et al. 2016). This has prompted
70 questions about whether such floods are 'caused' by climate change.

71 While no single weather or flood event can be directly attributed to anthropogenic
72 emissions of greenhouse gases, it is possible to assess how the chance of occurrence has
73 been altered by emissions, via probabilistic event attribution (PEA; Allen 2003). This
74 involves the generation of large ensembles of climate models runs, representing the
75 climate both as it is now and as it could have been had no past anthropogenic emissions
76 occurred. Data from the climate model runs can be analysed directly to investigate
77 weather events (e.g. England and Wales wet summers, Otto et al. 2015; UK cold winter
78 2010/11, Christidis and Stott 2012), but to investigate a flood event the climate
79 ensembles are used to drive a hydrological model to simulate runoff or river flow.
80 Application of PEA to the Autumn 2000 floods suggested that emissions had increased
81 the chance of occurrence, although with large uncertainty in the amount of increase and
82 variation in the effect on different catchments (Pall et al. 2011, Kay et al. 2011).

83 In the winter of 2013/14 a series of severe storms led to widespread and persistent
84 flooding across southern England, particularly the Somerset Levels and the lower
85 reaches of the River Thames (CEH 2014). Using PEA, Schaller et al. (2016) showed
86 that anthropogenic emissions gave an increase in January 2014 precipitation over
87 southern England of up to 0.5mm/day in the wettest 1% of the ensemble simulations.
88 This was shown to be due to both large-scale warming (the ability of warmer air to hold
89 more moisture) and local dynamical changes (an increase in the number of January days
90 with a westerly airflow), in the ratio of approximately 2/3 to 1/3; a result confirmed by
91 Vautard et al. (2016) using a different method. Catchment-based hydrological
92 modelling then showed that the rainfall changes led to an increase in 30-day mean flows
93 in the River Thames at Kingston (its most downstream flow gauge), although changes
94 in daily mean flows were much less. Flood risk mapping then showed a small increase

95 in the number of properties at risk of fluvial flooding in the Thames catchment. There
96 was a substantial range of numerical uncertainty in these analyses, reflecting weather
97 variability and climate model uncertainty. Further epistemic uncertainty, relating to
98 approximations made in the analysis of flood impacts, was acknowledged but not
99 quantified.

100 The catchment-based PEA study of Kay et al. (2011) showed that it is important to
101 account for variation in catchment response, due to spatial variation in physical
102 catchment properties. Spatial variation in rainfall can also be important, as shown by a
103 PEA analysis of the rainfall that led to flooding in December 2015
104 ([http://www.climateprediction.net/weatherathome/2015-december-extreme-weather-in-](http://www.climateprediction.net/weatherathome/2015-december-extreme-weather-in-the-uk/weatherhome-analysis/)
105 [the-uk/weatherhome-analysis/](http://www.climateprediction.net/weatherathome/2015-december-extreme-weather-in-the-uk/weatherhome-analysis/)), which gives different results over central and northern
106 England. Schaller et al. (2016) acknowledge that impacts on Winter 2103/14 flows and
107 damages for other rivers than the Thames are likely to differ because of variation in
108 catchment properties and spatial rainfall patterns.

109 The work presented here uses a national-scale grid-based hydrological model to
110 investigate spatial aspects of the Winter 2013/14 floods, based on the same climate
111 ensembles used by Schaller et al. (2016). The first part of the paper investigates river
112 flows across the whole of Britain using the grid-based hydrological model, looking at
113 the role of snow and providing a first national scale hydrological PEA analysis for the
114 nationally-significant Winter 2013/14 events. The second part re-investigates the
115 Thames basin, looking at both river flows and damage estimates and comparing results
116 to those from the catchment-based modelling of Schaller et al. (2016). Schaller et al.
117 (2016) was the first PEA study to express attributable risk in terms of the eventual
118 impacts of flooding, represented by the number of properties affected. To make that

119 analysis possible using the available hydrological model simulations, which were for
120 one location on the Thames (Kingston), it was assumed that the impacts throughout the
121 9,948 km² upstream catchment could be determined from the peak flow at Kingston.
122 Although this approximation was lent some support through consideration of the strong
123 spatial and temporal dependence within flood events on the Thames, it is generally
124 more realistic to assess flood impacts using a spatially-distributed analysis of peak
125 flows, inundation and the built environment. Spatially-distributed flood impacts
126 modelling has therefore been applied here for the first time in a PEA study; an
127 important advance that brings the analysis into line with the high level of detail
128 considered in models applied for re/insurance and infrastructure planning. A further
129 advance is that the new analysis accounts for the influence of flood defences.

130 **2 Background and Methodology**

131 **2.1 Winter 2013/14 flooding in Britain**

132 The meteorological review of Kendon and McCarthy (2015) describes a sequence of
133 storms affecting Britain between mid-December 2013 and mid-February 2014, with a
134 brief period of less stormy but still unsettled weather in mid-January. The storms
135 resulted in the wettest winter (December–February) in Britain since records began,
136 whether measured regionally using gridded precipitation from 1910, or using the
137 average England and Wales precipitation series from 1766. Within this, England
138 experienced its wettest January since records began.

139 The hydrological review of Muchan et al. (2015), based on data from 104 river flow
140 gauging stations across the UK (index rivers) covered by the National Hydrological
141 Monitoring Program (nrfa.ceh.ac.uk/nhmp), describes how flows were generally

142 declining and below the seasonal average in early December 2013 but increased quickly
143 in some responsive catchments as the storms began in mid-December. Floodplain
144 inundations became more widespread from the end of December, and flows in many
145 rivers in southern, central and eastern England increased substantially in January.
146 Further storms in early February led to further increases in flows, with 500 flood
147 warnings/alerts issued in England and Wales. Over the winter, a majority of index rivers
148 saw total flows exceeding previous winter records, but with few record peak flows;
149 overall, the winter was more exceptional for the duration of the high flows and
150 inundations.

151 This is confirmed by a wider analysis of gauged flow data from the National River Flow
152 Archive (nrfa.ceh.ac.uk), looking at the rankings of the maximum observed flows for
153 Winter 2013/14 for gauges with at least 40 years of relatively complete data up to 2014
154 (Figure 1). This shows that, while some catchments did experience record or near-
155 record peaks in daily mean flow during Winter 2013/14, many more catchments
156 experienced record flows at longer durations. Figure 1 also highlights the areas most
157 affected by flooding in Winter 2013/14, which reflect those areas experiencing the
158 highest rainfall totals over the period (Kendon and McCarthy 2015). The Somerset
159 Levels were particularly badly affected, with about 65km² flooded and a number of
160 villages cut off for a long period (Muchan et al. 2015, Willis and Fitton 2016). There
161 was also extensive and sustained flooding in the middle and lower Thames (Muchan et
162 al. 2015, Huntingford et al. 2014). According to the Association of British Insurers,
163 between 23 December 2013 and 28 February 2014 there were 18,700 flood insurance
164 claims totalling £451m, about half of which was for homes (ABI 2014). According to
165 Thorne (2014), “the number of properties inundated was surprisingly small given the

166 number and severity of the storms... [but] the societal impacts... were
167 disproportionately large”.

168 **2.2 Hydrological model**

169 The national-scale grid-based hydrological model CLASSIC-GB was developed by
170 combining the runoff-production scheme from the semi-distributed catchment-based
171 model CLASSIC (Climate and LAnd-use Scenario Simulation In Catchments; Crooks
172 and Naden 2007) in a modular framework with a kinematic wave routing module and
173 other modules like a temperature-based snow module (Crooks et al. 2014). CLASSIC
174 was used in the flood attribution studies of Schaller et al. (2016) and Kay et al. (2011),
175 and has been used to investigate the impacts of climate change on floods in catchments
176 across Britain (Prudhomme et al. 2013a,b, Kay and Crooks 2014).

177 CLASSIC-GB requires gridded input time-series of precipitation and potential
178 evaporation (PE), plus temperature (if the snow module is implemented), and can run at
179 spatial resolutions of 1km, 2.5km, 5km or 10km, aligned with the GB National Grid.
180 The routing time-step must be sufficiently short (relative to the spatial resolution) for
181 stability of the routing scheme, but the main model time-step can be a multiple of the
182 routing time-step. Here, CLASSIC-GB uses a 5km spatial resolution, 1-day main time-
183 step and 2-hour routing time-step. Runs at coarser spatial and temporal resolutions are
184 much faster, enabling use of large driving data ensembles (Section 2.3).

185 Crooks et al. (2014) tested CLASSIC-GB performance for 54 catchments (representing
186 a range of catchment types), using three measures of fit between simulated and observed
187 river flows. Analyses showed generally very good performance across the full range of
188 catchments. While performance was often better at finer resolutions, improvements

189 when moving from 5km to 1km resolution were generally small, so using the 5km
190 resolution is a good compromise between model performance and speed. Kay et al.
191 (2015) also analysed CLASSIC-GB performance (1km resolution), for 32 catchment
192 across southern Britain, using four measures of fit between flow statistics. Analyses
193 showed generally good performance, with that for high flows and flood frequency
194 showing no evidence of bias with respect to catchment properties (area, average annual
195 rainfall, altitude or baseflow index) but a tendency towards under-estimation in
196 catchments in south-west England. This tendency should be borne in mind, but is not
197 considered crucial for flood attribution analysis, which considers differences rather than
198 absolute values.

199 **2.3 Winter 2013/14 climate ensemble data**

200 Ensembles of climate data for December 2013 – February 2014 were produced using
201 the weather@home project (Massey et al. 2015), by running the HadRM3P Regional
202 Climate Model (RCM) for Europe (~50km resolution) nested in the HadAM3P
203 atmospheric Global Climate Model (GCM) driven with prescribed sea surface
204 temperatures (SSTs) and sea ice concentration (SIC). Initial conditions are perturbed
205 slightly for each ensemble member, to give a different realisation of the winter weather
206 and so account for natural variability. One ensemble represents the possible weather
207 under the current climate, using observed greenhouse gas concentrations, SSTs and SIC
208 for 2013/14 (“Actual”, named by the letter ‘a’). A further 11 ensembles represent the
209 possible weather had past anthropogenic emissions not occurred (“Natural”, named ‘e’
210 to ‘o’). These use pre-industrial atmospheric composition, the maximum well-observed
211 SIC, and estimates of pre-industrial SSTs constructed by subtracting anthropogenic SST
212 change patterns from observed SSTs. To account for uncertainty in estimated pre-

213 industrial SSTs, 11 patterns of SST change were applied based on GCM simulations
214 from CMIP5. Table 1 summarises the ensembles; see Schaller et al. (2016) for further
215 details.

216 The RCM runs provide the daily precipitation and temperature data required to drive
217 CLASSIC-GB, but do not provide PE, which has instead been estimated from monthly
218 mean temperature using the method of Oudin et al. (2005). Precipitation and PE are
219 then converted from the rotated latitude-longitude RCM grid to the 5km CLASSIC-GB
220 grid using area-weighting, with extra weighting based on standard average annual
221 rainfall patterns for precipitation (Kay et al. 2006). Temperature data are lapsed to the
222 CLASSIC-GB grid using altitude information.

223 CLASSIC-GB is then run with driving data from each ensemble member. To allow
224 spin-up of stores, runs are started in January 2010 using observed driving data; 1km
225 daily precipitation from CEH-GEAR (Tanguy et al. 2015, Keller et al. 2015), 5km Met
226 Office daily minimum and maximum temperature (Jenkins et al. 2008), and 40km
227 monthly PE from MORECS (Hough and Jones 1997). Observed data are used up to 10
228 December 2013, followed by RCM data from 11 December 2013; the first 10 days of
229 the RCM simulations are not used, to allow the atmosphere to spin up (precipitation in
230 the first few days of the Natural simulations is unrealistically high, but has stabilised
231 after 10 days – see Schaller et al (2016) for further detail). CLASSIC-GB was run both
232 with and without the snow module, to investigate the effects of snow.

233 ***2.4 Data analysis and damage estimation***

234 From each CLASSIC-GB run, the gridded daily mean flows for 11 December 2013 to
235 end February 2014 are extracted. To analyse flow peaks at a range of durations, the

236 daily time-series for each grid cell are turned into running mean flows for a range of
237 durations (10, 30 and 60 days) and the maximum flow extracted in each case.

238 The flow maxima are then used to estimate the Fraction of Attributable Risk, $FAR = I -$
239 NE/AE , where AE is the fraction of Actual runs with peak flows exceeding a given
240 threshold, and NE is the fraction of Natural runs with peak flows exceeding the
241 threshold (Allen 2003). A positive FAR indicates that past emissions have increased the
242 chance of peak river flows exceeding the chosen threshold (with a value of 1 suggesting
243 that exceedances may not have occurred without anthropogenic emissions), whereas a
244 negative FAR indicates that emissions have decreased the chance of peak river flows
245 exceeding the threshold. FAR is calculated for each Natural ensemble 'e' to 'o'
246 separately, and for a pooled Natural ensemble ('e-o', giving all members of each
247 separate Natural ensemble equal weight), relative to the threshold given by the 100-year
248 return period flow as simulated by the Actual ensemble. Similarly, FAR is calculated
249 for rainfall accumulations over a range of durations. Regional summaries use the eight
250 areas shown in Figure 3b, which are groupings of river basins based on the Water
251 Framework Directive River Basin Districts.

252 To estimate property damage within the catchment of the Thames at Kingston, peak
253 river flow data simulated using CLASSIC-GB were fed into a model combining flood
254 inundation extents, depths and property locations. This model is a subset of the JBA
255 Risk Management UK Flood Probabilistic Model (JBA Risk Management 2015), which
256 is one of several models used by the insurance industry, and has been adopted by the
257 state-mandated reinsurance scheme Flood Re (Insurance Journal 2015) to provide
258 estimates of damage and financial loss for flood events. It is (in common with
259 comparable products) a proprietary model, however the foundations of the approach are

260 detailed (5m x 5m cell resolution) inundation mapping based on 2D hydrodynamic
261 modelling, using peer-reviewed methodologies that were summarised by Schaller et al.
262 (2016).

263 For each ensemble member simulated using CLASSIC-GB, the peak flow values are
264 interpolated spatially to a set of points placed on the river network. Each peak flow
265 value needs to be represented as an inundation extent and depth in every postcode unit
266 within the Thames catchment. To do this without needing to hydraulically model
267 floodplain inundation for each ensemble member (which would be computationally
268 very expensive) a set of five pre-modelled design floods representing annual
269 exceedance probabilities from 1/20 to 1/1000 are used. The peak flows are converted to
270 return periods, spatially interpolated to the postcode units and then extents and depths at
271 each postcode unit are interpolated from the pre-modelled design floods. This approach
272 is analogous to the development of a river flood ‘catastrophe model’ applied for
273 estimation of risk across an insured portfolio (see Toothill and Lamb 2017, Figure 3.15,
274 for a summary).

275 To estimate the number of properties affected in each postcode unit, the Thames subset
276 model includes an input property dataset; developed using population data from the UK
277 census (ONS 2011) combined with property location data purchased from a commercial
278 provider (Rightmove) containing 3.4 million residential properties. Each property is
279 attributed with a postcode unit but the exact footprint of an individual building is not
280 known. This is recognised to be an important source of uncertainty in flood risk
281 assessments (e.g. when comparing flood model predictions with insurance claims data)
282 because even relatively small scale positional uncertainties can affect the number of
283 properties calculated as being within a flooded area, especially at the margins of

284 flooding in densely populated locations. To overcome this, for each individual property
285 and for every ensemble member, many samples are drawn from range of water depths
286 within that postcode unit. This also accounts for the proportion of the postcode that is
287 predicted to be dry. A property is counted as being flooded if the mean of the sampled
288 depths is greater than 20cm. Flood defence information is included; properties in areas
289 benefiting from flood defences are only assumed to flood if the peak river flow exceeds
290 the standard of protection of the associated flood defence.

291 **3 Results**

292 **3.1 National**

293 Maps show that flow FAR values calculated from the pooled Natural ensemble ('e-o')
294 vary considerably across Britain, particularly for shorter duration peak flows (Figure 2).
295 For daily peak flows, parts of south-east England show negative FAR while much of
296 western England, Wales and Scotland show positive FAR. For 10-day peak flows, FAR
297 values for parts of north-east England are strongly negative ($FAR < 0.5$), whereas FAR
298 values are positive for much of the rest of the country (apart from small parts of south-
299 east England, Wales and south-west Scotland for example). For 30-day peak flows,
300 FAR in north-east England is less strongly negative and there are even fewer negative
301 FAR values elsewhere. For 60-day peak flows, FAR in parts of north-east England is
302 still slightly negative but FAR is positive almost everywhere else (apart from a few
303 pixels to the far eastern side of Scotland). In general, FARs are higher for longer
304 durations than for shorter durations.

305 Boxplots summarising the FAR values calculated from the pooled Natural ensemble ('e-
306 o') highlight the variation in values between different regions of the country (Figure 3).

307 They also illustrate that there is little variation in FAR within some regions (especially
308 in southern England), but a much wider range of FAR in other regions (especially
309 Scotland and northern England).

310 For parts of eastern Scotland, FAR is strongly positive (>0.5) for all durations (Figure 2
311 and Figure 3). This is related to changes in flow patterns associated with changes in
312 snowfall and snowmelt in this Highland region, which is one of the few areas of Britain
313 that experiences significant annual snowfall even today (Kay 2016). When modelled
314 without the snow module, these positive FAR are significantly reduced, becoming
315 negative for longer durations (Figure 3 and Figure 4). A study of future potential
316 changes in peak flows under climate change also highlighted this region of Britain as
317 one where changes in snow were likely to have a significant effect on the expected
318 changes in flows (Bell et al. 2016). Although the influence of snow is largest in eastern
319 Scotland and at longer durations, it also has an effect in more southerly regions (e.g.
320 Anglian, SE England and W England) at shorter durations (1- and 10-day), where FAR
321 is typically lower when modelled with snow than without. This was previously shown
322 for the Thames at Kingston (Schaller et al. 2016), and suggests that snow changes are
323 moderating the increases in shorter duration peak flows.

324 Boxplots summarising the FAR values calculated from each Natural ensemble 'e' to 'o'
325 separately (Figure 5) highlight the large variation between them. The same natural
326 ensemble ('m') leads to the highest median FAR value across most regions for all
327 durations, the exceptions being regions in the south and west, where ensemble 'f' gives
328 higher FAR at the 10-day duration and ensemble 'g' gives marginally higher FAR at the
329 60-day duration. The natural ensemble with the lowest median FAR value varies more
330 between regions. Ensemble 'n' generally gives the lowest FAR in regions towards the

331 south and east (SE England, Anglian and NE England), and ensemble 'l' generally gives
332 the lowest FAR in north-western regions (NW England and most of Scotland). In south-
333 western regions (SW England, W England and E Wales) ensembles 'h', 'j' and 'l' all
334 give similarly low FAR values for durations of 1, 10 and 30 days, but ensemble 'j' gives
335 the lowest FAR for the 60-day duration.

336 Comparing the estimated FAR values across Britain (Figure 2) with the rankings of
337 observed Winter 2013/14 flows (Figure 1) shows some similarities, in that the FAR
338 values are generally greater for longer durations and the observed flows were more
339 record-breaking at longer durations. However, there appears to be little spatial
340 consistency, especially for daily mean flows: Some areas with positive FARs
341 experienced few record flows (e.g. the far south-west of England, Wales and Scotland)
342 while some areas with negative FARs experienced a number of record flows (e.g. south-
343 east England). While Schaller et al. (2016) showed that the RCM driven by observed
344 boundary conditions was able to represent the large-scale situation of the event
345 reasonably well, these results indicate that the average RCM response in terms of
346 precipitation was different compared to what happened in reality. This is unsurprising as
347 there is only one 'realisation' from the weather in the real world, but a distribution of
348 realisations in the model ensembles.

349 Maps of precipitation FAR (Figure 6) are relatively consistent with those for flow FAR
350 (Figure 2 and Figure 4), in that precipitation FAR values are also generally greater for
351 longer durations, and there is a good amount of spatial consistency. However, for most
352 river points, precipitation FARs are higher than flow FARs for the same duration
353 (Figure 7), reflecting the complexity of the transformation of precipitation into river
354 flows. Similarly, the generally lower correlation between flow and precipitation FARs

355 at the 1-day duration reflects the fact that different catchments, with different physical
356 properties (e.g. area, orientation, geology), respond in different ways to the same
357 climatic inputs, so a high increase in 1-day rainfall in a small ‘flashy’ responsive
358 catchment can cause a high increase in daily peak flow, but to get the same increase in
359 daily peak flow in a more slowly responding catchment would require a more sustained
360 increase in rainfall, typically over a number of days. In particular, the presence of
361 groundwater and its influence in attenuating catchment responses to precipitation is
362 likely to be important in parts of southern and eastern England.

363 In north-western and eastern Scotland, correlations between precipitation and flow
364 FARs are generally lower than for other regions, even for higher durations, and flow
365 FARs can be much higher than precipitation FARs in some cases, especially at longer
366 durations (Figure 7). This is again because of the influence of extended periods of snow
367 accumulation and melt in these more northerly, typically higher altitude, colder regions;
368 correlations are much higher when flows are simulated without the snow module (not
369 shown).

370 **3.2 *Thames at Kingston***

371 The maps in Figure 8 show the spatial variation in FAR calculated for peak daily flows
372 across the catchment of the Thames at Kingston, and the variation between the 11
373 natural ensembles. Table 2 summarises the FAR values for the catchment, in terms of
374 the value at the outlet point and the minimum and maximum values across the whole
375 catchment, for the pooled natural ensemble (‘e-o’) and for each natural ensemble (‘e’ to
376 ‘o’) separately. Table 2 also shows the FAR values for the outlet point estimated from
377 the catchment-based modelling of Schaller et al. (2016). For some natural ensembles the

378 outlet FAR from the gridded modelling is higher than that from the catchment-based
379 modelling, but for other ensembles the opposite is true. This includes the pooled natural
380 ensemble ('e-o'), for which the outlet FAR value is 0.004 from the gridded modelling
381 but 0.032 from the catchment-based modelling (although with resampling the 5th-95th
382 percentile range from the latter was -0.117 to 0.146, so the new value is well within the
383 uncertainty range).

384 The gridded modelling shows that FAR values upstream in the Thames can be much
385 higher than at the outlet (Figure 8 and Table 2). For the pooled natural ensemble ('e-o')
386 FAR goes up to 0.186, although some tributaries closer to the outlet at Kingston have
387 negative FAR values (down to -0.142). This suggests that damages estimated using
388 gridded modelling should be more reliable than assuming that what happens at the
389 outlet point is representative of the whole catchment (as done by Schaller et al. 2016).

390 Figure 9 maps the FAR calculated for counts of flooded residential properties
391 aggregated into the 395 postcode districts within the catchment, each of which contains
392 between 2 and 38,733 properties (average 8,774). The results are consistent with the
393 analysis of peak flows: For the pooled ensemble, FAR for flooded properties is greater
394 than zero across much of the catchment, but there are some districts with values below
395 zero. As with the peak flows (Figure 8), the spatial patterns of FAR for flooded
396 properties exhibit considerable variation between ensembles, with some ensembles
397 containing districts for which the FAR indicates considerably stronger influence of past
398 emissions on flood risk, either in terms of an increase or a decrease in likelihood of
399 flooding.

400 Whilst the FAR results indicate, overall, a slightly increased likelihood of flooding
401 connected with past greenhouse gas emissions, Figure 10 shows the magnitude and

402 uncertainty of this increase in attributable risk, expressed in terms of the difference
403 between the number of properties flooded in the Actual ensemble and each Natural
404 ensemble, and plotted as a function of increasing levels of extremeness within the
405 ensembles (interpreted as a return period in years). A comparable result was presented
406 by Schaller et al. (2016; Figure 5f), based on the simplifying assumption of spatial
407 uniformity, and their headline estimate of 1,000 additional properties at risk is also
408 shown in Figure 10. The new results show an increase, attributable to past emissions, in
409 the number of properties at risk of flooding over a wide range of event magnitudes
410 ranging from 20- to 500-year return periods (conditional on the ensemble simulations).
411 This result is broadly consistent with the earlier analysis of Schaller et al. (2016), but
412 with some important refinements stemming from the new, distributed impacts analysis.
413 Firstly, the quantum of the increase in attributable risk is smaller than the previous
414 findings, but also within a narrower range of uncertainty. The mean of the pooled
415 ensemble increase (calculated over the range of return periods in Figure 10) is +457
416 properties, with the individual ensembles ranging between -1,334 (ensemble 'n') and
417 +4,605 (ensemble 'o'). This can be compared with Schaller et al. (2016) estimates of
418 approximately -4,000 to +8,000.

419 Secondly, whilst there is some variation in the number of properties at additional risk
420 over the range of return periods, both here and in Schaller et al. (2016), the new analysis
421 shows a coherent reduction in the quantum of attributable risk (for the pooled ensemble)
422 for return periods between 50 and 400 years, with almost no change attributable to past
423 emissions for return periods between 100 to 300 years. This reduction is observed in
424 most, though not all, of the individual ensembles. It reflects the expected influence of
425 flood defences in the impacts analysis: an increase in river flows will not translate to

426 more properties being flooded if those flows are still contained by flood defence
427 systems. Only a small proportion of properties in the catchment benefit from significant
428 flood defences (see Schaller et al. (2016) Supplementary Information), and hence flood
429 defences have no influence on attributable risk in many parts of the catchment.
430 However, where defences do exist their marginal influence could be significant. This
431 effect is expected to be felt for events that are similar in severity, or somewhat less
432 severe, than the standard of protection of the defence systems, which are typically
433 designed to resist flood flows no worse than a 200-year return period in the Thames
434 catchment (Environment Agency, 2009). For events that are sufficiently extreme to
435 exceed flood defence standards, the marginal influence of those defences (i.e. for an
436 incremental increase in river flow) should diminish. Although the return period scale in
437 Figure 10 is not defined in precisely the same way as the standard of protection of flood
438 defences (owing to the conditional nature of return periods calculated within the
439 simulated ensemble), the pattern in Figure 10 is consistent with the expected influence
440 of flood defences as discussed above.

441 **4 Discussion and Conclusions**

442 The seemingly high incidence of floods in Britain in recent years has prompted
443 increasing questions about the role of climate change. Thus methods like probabilistic
444 event attribution, that can assess the influence of anthropogenic emissions on event
445 occurrence, are becomingly increasingly important. Here, large ensembles of climate
446 model runs, representing both Actual and Natural conditions, have been used to drive a
447 national-scale hydrological model, to assess the influence of emissions on the Winter
448 2013/14 floods. The results show that emissions are likely to have increased the chance
449 of occurrence of these floods across much of the country ($FAR > 0$; Figure 2), with the

450 influence on longer duration peaks being greater than that for shorter durations. This is
451 consistent with an analysis of observed flows for the period (Figure 1), which shows
452 that they were more unusual (relative to flows over the preceding 40+ years) at longer
453 durations.

454 Analyses of flow FAR produced with and without the snow module (Figure 3) show
455 that changes in snow processes are affecting flows differently in different parts of the
456 country. In more northerly regions snow changes are increasing FAR, especially at
457 longer durations, but in more southerly regions and for shorter durations they are
458 decreasing FAR. This highlights the importance of using hydrological modelling, as
459 analyses of precipitation totals do not allow for changes in snowfall and snowmelt.

460 While flow FAR and precipitation FAR patterns are relatively consistent (especially
461 when the hydrological model is run without the snow module), the precipitation FAR
462 are often higher than the flow FAR, and the correlation between the two varies by
463 region and by duration (Figure 7). This again highlights the importance of using
464 hydrological modelling to attribute hydrological impacts from meteorological changes,
465 to incorporate the complexities of the transformation of precipitation into runoff and
466 river flow. There is variation in the response of different rivers not just because of
467 spatial variation in rainfall patterns but because of variation in physical properties that
468 influence runoff production.

469 Similar variation is also visible when the change in risk attributable to past greenhouse
470 gas emissions is translated from the hydro-meteorological domain into impacts of
471 flooding on properties (Figure 9). This variation in patterns of attributable risk can only
472 be explored by using a distributed modelling approach, linking spatially-varying
473 hydrological simulations to detailed, spatially explicit inundation and impacts analysis.

474 Here, such an approach has been demonstrated for the Thames catchment, applying
475 state-of-the-art industry models for flood inundation and impacts analysis, which also
476 include flood defences. Over a range of possible events of increasing severity, the
477 combined modelling suggests a central estimate of +457 properties placed at additional
478 risk because of historical greenhouse gas emissions, within an uncertainty range
479 of -1,334 to +4,605. This figure refines earlier estimates of ~1,000 additional properties
480 at risk (range -4,000 to +8,000), with a consistent interpretation that the balance of
481 probabilities indicates an increase in risk attributable to climate change. The attributable
482 change in risk of property flooding varies with the relative severity of events within the
483 ensemble simulation. This variation appears to be in line with the expected influence of
484 flood defences. Flood defences may be able to “absorb” some of the additional risk
485 attributed to climate change, but cannot be relied upon to do so for extreme events,
486 which are nevertheless now shown to be somewhat more likely in the present-day
487 climate than they would have been under pre-industrial conditions.

488 Uncertainty related to the day-to-day variation in the weather is accounted for through
489 an ensemble approach, with uncertainty in pre-industrial SSTs accounted for through
490 use of SST changes from a range of climate models, resulting in a wide range of FAR
491 values. However, only one GCM/RCM was used for the climate simulations, with one
492 hydrological model; other models may give different results (as for future climate
493 change impacts; e.g. Kay et al. 2009). Ideally a range of climate models would be
494 applied, as this is likely to be the largest source of uncertainty (Vetter et al. 2017, Kay et
495 al. 2009), although using a higher resolution GCM could avoid the need for a nested
496 RCM. Uncertainties in the flood inundation mapping and the sub-postcode location of
497 properties are accounted for via a sampling approach. Flood defences are included,

498 although uncertainties about their actual (as opposed to design) standards and potential
499 for structural failures (e.g. breaching) have not been explored.

500 While the results presented here and in Schaller et al. (2016) suggest that past
501 anthropogenic greenhouse gas emissions have led to an increased chance of flooding
502 from weather events like those experienced in Winter 2013/14, caution needs to be
503 exercised when inferring how future changes will develop. The modelling study of
504 Rasmijn et al. (2016) suggests that, in a future warmer climate, further changes in
505 atmospheric dynamics will counterbalance the increased atmospheric moisture content,
506 leading to similar precipitation anomalies for the Winter 2013/14 event in the future as
507 in the present day. However, they also suggest that the circulation anomaly of Winter
508 2013/14 may occur more frequently in future, meaning a likely continued increase in
509 flood risk (unless additional mitigation/adaptation is implemented). This demonstrates
510 the complex and large-scale effects of the atmospheric interactions involved, alongside
511 the complexities of the hydrological processes that transform precipitation into runoff
512 and river flow. Thus detailed and proven climate models and hydrological models are
513 required, along with inundation and damage models, to reliably investigate climate-
514 driven changes in floods and their impacts on people.

515 **Acknowledgements**

516 AK was supported by the NERC/CEH Water and Pollution Science programme. RL
517 was supported by JBA Trust project W14-7574. NS was supported by EUCLEIA (EU
518 FP7 grant 607085). We thank the volunteers who donated computing time to
519 weather@home.

520 **References**

- 521 ABI. 2014. 2014 floods: the numbers [[https://www.abi.org.uk/Insurance-and-](https://www.abi.org.uk/Insurance-and-savings/Topics-and-issues/Flooding/Flooding-in-numbers/2014-floods-in-numbers)
522 [savings/Topics-and-issues/Flooding/Flooding-in-numbers/2014-floods-in-numbers;](https://www.abi.org.uk/Insurance-and-savings/Topics-and-issues/Flooding/Flooding-in-numbers/2014-floods-in-numbers)
523 last accessed October 2016]
- 524 Allen M. 2003. Liability for climate change, *Nature*, 421, 891–892.
- 525 Barker L, Hannaford J, Muchan K, Turner S, Parry S. 2016. The winter 2015/2016
526 floods in the UK: a hydrological appraisal. *Weather*, 71(12), 324-333.
- 527 Bell VA, Kay AL, Davies HN, Jones RG. 2016. An assessment of the possible
528 impacts of climate change on snow and peak river flows across Britain. *Climatic*
529 *Change*, 136(3), 539–553.
- 530 Blöschl G, Hall J, Parajka J, Perdigão RAP, Merz B, Arheimer B, Aronica GT,
531 Bilibashi A, Bonacci O, Borga M, Čanjevac IO, Castellarin A, Chirico GB, Claps P,
532 Fiala K, Frolova N, Gorbachova L, Gül A, Hannaford J, Harrigan S, Kireeva M,
533 Kiss A, Kjeldsen TR, Kohnová S, Koskela JJ, Ledvinka O, Macdonald N, Mavrova-
534 Guirguinova M, Mediero L, Merz R, Molnar P, Montanari A, Murphy C, Osuch M,
535 Ovcharuk V, Radevski I, Rogger M, Salinas JL, Sauquet E, Šraj M, Szolgay J,
536 Viglione A, Volpi E, Wilson D, Zaimi K, Živković N. 2017. Changing climate
537 shifts timing of European floods. *Science*, 357(6351), 588-590,
538 doi:10.1126/science.aan2506
- 539 CEH. 2014. Hydrological Summary for the United Kingdom: February 2014.
540 Centre for Ecology & Hydrology, 12pp.
- 541 Christidis N, Stott P. 2012. Lengthened odds of the cold UK winter of 2010/11
542 attributable to human influence. *B. Am. Meteorol. Soc.*, 93(7), 1060-1062.

- 543 Crooks SM, Kay AL, Davies HN, Bell VA. 2014. From Catchment to National
544 Scale Rainfall-Runoff Modelling: Demonstration of a Hydrological Modelling
545 Framework. *Hydrology*, 1(1), 63–88.
- 546 Crooks SM, Naden PS. 2007. CLASSIC: a semi-distributed modelling system. *Hydrol.*
547 *Earth Syst. Sci.*, 11, 516–531.
- 548 Environment Agency. 2009. Thames Catchment Flood Management Plan. ref: LIT
549 4403, GETH1209BQYL-E-E, Bristol, UK.
- 550 Hannaford J. 2015. Climate-driven changes in UK river flows: A review of the
551 evidence. *Prog. Phys. Geogr.*, 39(1), 29–48.
- 552 Hough M, Jones RJA. 1997. The United Kingdom Meteorological Office rainfall and
553 evaporation calculation system: MORECS version 2.0 — an overview. *Hydrol. Earth*
554 *Syst. Sci.*, 1, 227–239.
- 555 Huntingford C, Marsh T, Scaife AA, Kendon EJ, Hannaford J, Kay AL, Lockwood M,
556 Prudhomme C, Reynard NS, Parry S, Lowe JA, Screen JA, Ward HC, Roberts M, Stott
557 PA, Bell VA, Bailey M, Jenkins A, Legg T, Otto FEL, Massey N, Schaller N, Slingo J,
558 Allen MR. 2014. Potential influences in the United Kingdom's floods of winter 2013-
559 14. *Nature Climate Change*, 4(9), 769–777.
- 560 Insurance Journal. 2015. JBA Releases Comprehensive UK Flood Model before Flood
561 Re Launch. Available at:
562 www.insurancejournal.com/news/international/2015/12/18/392460.htm, accessed 18
563 December 2015.

- 564 JBA Risk Management. 2015. JBA Risk Management releases comprehensive new UK
565 flood model for Flood Re. Available at: [www.jbarisk.com/jba-risk-management-](http://www.jbarisk.com/jba-risk-management-releases-comprehensive-new-uk-flood-model-flood-re)
566 [releases-comprehensive-new-uk-flood-model-flood-re](http://www.jbarisk.com/jba-risk-management-releases-comprehensive-new-uk-flood-model-flood-re), accessed 18 December 2015.
- 567 Jenkins GJ, Perry MC, Prior MJ. 2008. The climate of the United Kingdom and recent
568 trends. Met Office Hadley Centre, Exeter, UK.
- 569 Jiménez Cisneros BE, Oki T, Arnell NW, Benito G, Cogley JG, Döll P, Jiang T,
570 Mwakalila SS. 2014. Freshwater Resources. In: *Climate Change 2014: Impacts,*
571 *Adaptation, and Vulnerability. Part A: Global and Sectoral Aspects. Contribution of*
572 *Working Group II to the Fifth Assessment Report of the Intergovernmental Panel on*
573 *Climate Change* [Field CB, Barros VR et al. (eds.)]. CUP, Cambridge, UK and New
574 York, NY, USA, 229–269.
- 575 Kay AL. 2016. A review of snow in Britain: the historical picture and future
576 projections. *Prog. Phys. Geogr.*, 40(5) 676–698.
- 577 Kay AL, Bell VA, Blyth EM, Crooks SM, Davies HN, Reynard NS. 2013. A
578 hydrological perspective on evaporation: historical trends and future projections in
579 Britain. *J. Water Clim. Change*, 4(3), 193–208.
- 580 Kay AL, Crooks SM. 2014. An investigation of the effect of transient climate change on
581 snowmelt, flood frequency and timing in northern Britain. *Int. J. Climatol.*, 34, 3368–
582 3381.
- 583 Kay AL, Crooks SM, Pall P, Stone D. 2011. Attribution of Autumn/Winter 2000
584 flood risk in England to anthropogenic climate change: A catchment-based study. *J.*
585 *Hydrol.*, 406, 97–112.

- 586 Kay AL, Davies HN, Bell VA, Jones RG. 2009. Comparison of uncertainty sources
587 for climate change impacts: flood frequency in England. *Climatic Change*, 92(1–2),
588 41–63.
- 589 Kay AL, Reynard NS, Jones RG. 2006. RCM rainfall for UK flood frequency
590 estimation. I. Method and validation. *J. Hydrol.*, 318, 151–162.
- 591 Kay AL, Rudd AC, Davies H, Kendon EJ, Jones RG. 2015. Use of very high
592 resolution climate model data for hydrological modelling: baseline performance and
593 future flood changes. *Climatic Change*, 133(2), 193–208.
- 594 Keller VDJ, Tanguy M, Prosdocimi I, Terry JA, Hitt O, Cole SJ, Fry M, Morris DG,
595 Dixon H. 2015. CEH-GEAR: 1 km resolution daily and monthly areal rainfall estimates
596 for the UK for hydrological use. *Earth Syst. Sci. Data*, 7, 143–155.
- 597 Kendon M, McCarthy M. 2015. The UK's wet and stormy winter of 2013/2014.
598 *Weather*, 70(2), 40–47.
- 599 Massey N, Jones R, Otto FEL, Aina T, Wilson S, Murphy JM, Hassell D, Yamazaki
600 YH, Allen MR. 2015. weather@home - development and validation of a very large
601 ensemble modelling system for probabilistic event attribution. *Q.J.R. Meteorol.*
602 *Soc.*, 141, 1528–1545.
- 603 Muchan K, Lewis M, Hannaford J, Parry S. 2015. The winter storms of 2013/2014 in
604 the UK: hydrological responses and impacts. *Weather*, 70(2), 55–61.
- 605 Otto FEL, Rosier SM, Allen MR, Massey NR, Rye CJ, Quintana JI. 2015. Attribution
606 analysis of high precipitation events in summer in England and Wales over the last
607 decade. *Climatic Change*, 132, 77–91.

- 608 Oudin L, Hervieu F, Michel C, Perrin C, Andreassian V, Anctil F, Loumagne C. 2005.
609 Which potential evapotranspiration input for a lumped rainfall-runoff model? Part 2 —
610 Towards a simple and efficient potential evapotranspiration model for rainfall-runoff
611 modelling. *J. Hydrol.*, 303, 290–306.
- 612 Pall P, Aina T, Stone DA, Stott PA, Nozawa T, Hilberts AGJ, Lohmann D, Allen
613 MR. 2011. Anthropogenic greenhouse gas contribution to flood risk in England and
614 Wales in autumn 2000. *Nature*, 470, 382–385.
- 615 Prudhomme C, Crooks S, Kay AL, Reynard NS. 2013a. Climate change and river
616 flooding: Part 1 Classifying the sensitivity of British catchments. *Climatic Change*, 119,
617 933–948.
- 618 Prudhomme C, Haxton T, Crooks S, Jackson C, Barkwith A, Williamson J, Kelvin
619 J, Mackay J, Wang L, Young A, Watts G. 2013b. Future Flows Hydrology: an
620 ensemble of daily river flow and monthly groundwater levels for use for climate
621 change impact assessment across Great Britain. *Earth Syst. Sci. Data*, 5, 101–107.
- 622 Rasmijn LM, van der Schrier G, Barkmeijer J, Sterl A, Hazeleger W. 2016.
623 Simulating the extreme 2013/2014 winter in a future climate. *J. Geophys. Res.*
624 *Atmos.*, 121, 5680–5698.
- 625 Schaller N, Kay AL, Lamb R, Massey NR, van Oldenborgh GJ, Otto FEL, Sparrow
626 SN, Vautard R, Yiou P, Ashpole I, Bowery A, Crooks SM, Haustein K,
627 Huntingford C, Ingram WJ, Jones RG, Legg T, Miller J, Skeggs J, Wallom D,
628 Weisheimer A, Wilson S, Stott PA, Allen MR. 2016. Human influence on climate
629 in the 2014 Southern England winter floods and their impacts. *Nature Climate*
630 *Change*, 6(6), 627–634.

- 631 Toothill J, Lamb R. 2017. Inland Flooding, Chapter 3.5 in Mitchell-Wallace K,
632 Jones M, Hillier J, Foote M (Eds.), Natural Catastrophe Risk Management and
633 Modelling: A Practitioner's Guide. 1st edition, Wiley-Blackwell, pp.218-229.
- 634 Tanguy M, Dixon H, Prosdocimi I, Morris DG, Keller VDJ. 2015. Gridded
635 estimates of daily and monthly areal rainfall for the United Kingdom (1890-2014)
636 [CEH-GEAR]. NERC-EIDC, doi:10.5285/f2856ee8-da6e-4b67-bedb-590520c77b3c
- 637 Thorne C. 2014. Geographies of UK flooding in 2013/14. *The Geographical*
638 *Journal*, 180(4), 297–309.
- 639 Vautard R, Yiou P, Otto F, Stott P, Christidis N, van Oldenborgh GJ, Schaller N.
640 2016. Attribution of human-induced dynamical and thermodynamical contributions
641 in extreme weather events. *Environmental Research Letters*, 11(11), 114009.
- 642 Vetter T, Reinhardt J, Flörke M, van Griensven A, Hattermann F, Huang S, Koch
643 H, Pechlivanidis IG., Plötner S, Seidou O, Su B, Vervoort RW, Krysanova V. 2017.
644 Evaluation of sources of uncertainty in projected hydrological changes under
645 climate change in 12 large-scale river basins. *Climatic Change*, 141(3), 419–433
- 646 Watts G, Battarbee RW, Bloomfield JP, Crossman J, Daccache A, Durance I, Elliot
647 JA, Garner G, Hannaford J, Hannah DM, Hess T, Jackson CR, Kay AL, Kernan M,
648 Knox J, Mackay J, Monteith DT, Ormerod SJ, Rance J, Stuart ME, Wade AJ, Wade
649 SD, Weatherhead K, Whitehead PG, Wilby RL. 2015. Climate change and water in
650 the UK – past changes and future prospects. *Prog. Phys. Geogr.*, 39, 6–28.
- 651 Willis I, Fitton J. 2016. A review of multivariate social vulnerability
652 methodologies: a case study of the River Parrett catchment, UK. *Nat. Hazards Earth*
653 *Syst. Sci.*, 16, 1387–1399.

654

655 **Tables**656 **Table 1 Summary of the Actual and Natural climate ensembles for Winter 2013/14.**

| ID letter | Ensemble set | Number of members | SST source |
|-----------|--------------|-------------------|---------------------------------|
| a | Actual | 17220 | Observed |
| e | Natural | 7147 | Obs – CanESM Δ SST |
| f | Natural | 13823 | Obs – CCSM4 Δ SST |
| g | Natural | 7332 | Obs – CNRM-CM5 Δ SST |
| h | Natural | 7530 | Obs – CSIRO-Mk3 Δ SST |
| i | Natural | 15565 | Obs – GFDL-CM3 Δ SST |
| j | Natural | 15335 | Obs – GISS-E2-H Δ SST |
| k | Natural | 7159 | Obs – GISS-E2-R Δ SST |
| l | Natural | 10964 | Obs – HadGEM2-ES Δ SST |
| m | Natural | 7651 | Obs – IPSL-CM5A-LR Δ SST |
| n | Natural | 10177 | Obs – IPSL-CM5A-MR Δ SST |
| o | Natural | 13210 | Obs – MIROC-ESM Δ SST |

657

658 **Table 2 Summary of Thames@Kingston flow FAR values for Winter 2013/14,**
 659 **from the catchment-based modelling of Schaller et al. (2016) and from gridded**
 660 **modelling.**

| Natural ensemble | Schaller et al. outlet FAR | | FAR from gridded modelling | | |
|------------------|----------------------------|--|----------------------------|-------------------|-------------------|
| | Direct estimate | Resampling: median (5 th -95 th percentiles) | Outlet value | Catchment minimum | Catchment maximum |
| e-o (pooled) | 0.032 | 0.028 (-0.117 - 0.146) | 0.004 | -0.142 | 0.186 |
| e | 0.039 | 0.036 (-0.213 - 0.245) | 0.061 | -0.149 | 0.286 |
| f | 0.237 | 0.233 (0.060 - 0.377) | 0.182 | 0.001 | 0.377 |
| g | 0.226 | 0.222 (0.006 - 0.400) | 0.140 | -0.106 | 0.427 |
| h | -0.097 | -0.104 (-0.377 - 0.117) | 0.003 | -0.29 | 0.109 |
| i | 0.009 | 0.004 (-0.195 - 0.166) | -0.164 | -0.248 | 0.170 |
| j | -0.207 | -0.213 (-0.441 - -0.023) | -0.182 | -0.417 | 0.001 |
| k | 0.027 | 0.022 (-0.227 - 0.234) | 0.007 | -0.189 | 0.217 |
| l | -0.017 | -0.022 (-0.244 - 0.169) | -0.096 | -0.178 | 0.169 |
| m | 0.428 | 0.426 (0.250 - 0.571) | 0.372 | 0.097 | 0.542 |
| n | -0.193 | -0.200 (-0.456 - 0.020) | -0.121 | -0.554 | 0.115 |
| o | 0.073 | 0.069 (-0.130 - 0.235) | 0.091 | -0.243 | 0.348 |

661

662 **Figure captions**

663 **Figure 1 Maps showing the ranks of the maximum observed flows over December**
 664 **2013–February 2014, for 1-, 10-, 30- and 60-day mean flows, for 342 gauges with at**
 665 **least 40 years of available data up to 2014.**

666 **Figure 2 Maps of FAR values (using the pooled Natural ensemble), for 1-, 10-, 30-**
 667 **and 60-day mean flows.**

668 **Figure 3 a) Boxplots summarising the range of FAR values for eight regions across**
669 **Britain (using the pooled Natural ensemble), for 1-, 10-, 30- and 60-day mean**
670 **flows, when modelled with and without the snow modules. The boxes show the**
671 **25th-75th percentile range (with the black line showing the median), the whiskers**
672 **show the 5th and 95th percentiles, and additional markers show minima and**
673 **maxima. b) Region map.**

674 **Figure 4 As Figure 2 but simulated without the snow module.**

675 **Figure 5 Boxplots summarising the range of FAR values for eight regions across**
676 **Britain (Figure 3b) for 1-, 10-, 30- and 60-day mean flows, for the pooled Natural**
677 **ensemble ('e-o') and each Natural ensemble ('e' to 'o') separately (see key). The**
678 **boxes are defined as in Figure 3a.**

679 **Figure 6 Maps of precipitation FAR values (using the pooled Natural ensemble),**
680 **for 1-, 10-, 30- and 60-day accumulation periods.**

681 **Figure 7 Scatter plots of flow FAR versus precipitation FAR (using the pooled**
682 **Natural ensemble), for river points in eight regions across Britain (Figure 3b), for**
683 **1-, 10-, 30- and 60-day durations. The Pearson r correlation for each duration is**
684 **shown in the bottom-right of each plot.**

685 **Figure 8 Maps of FAR values for 1-day mean flows in the Thames@Kingston**
686 **catchment (black outline and dot), using the pooled Natural ensemble ('e-o') and**
687 **each Natural ensemble ('e' to 'o') separately.**

688 **Figure 9 As Figure 8 but for flooded properties in each postcode district of the**
689 **Thames@Kingston catchment.**

690 **Figure 10 Difference between number of properties flooded in the Actual ensemble**
691 **relative to the pooled Natural ensemble ('e-o') and each Natural ensemble ('e' to**
692 **'o') separately. Data are plotted as a function of relative level of extremeness**
693 **within the ensemble (interpreted as a return period in years). The dashed line**
694 **shows the estimate made by Schaller et al. (2016) under spatial uniformity**
695 **assumptions.**

696

Peer Review Only

Flood event attribution and damage estimation using national-scale grid-based modelling: Winter 2013/14

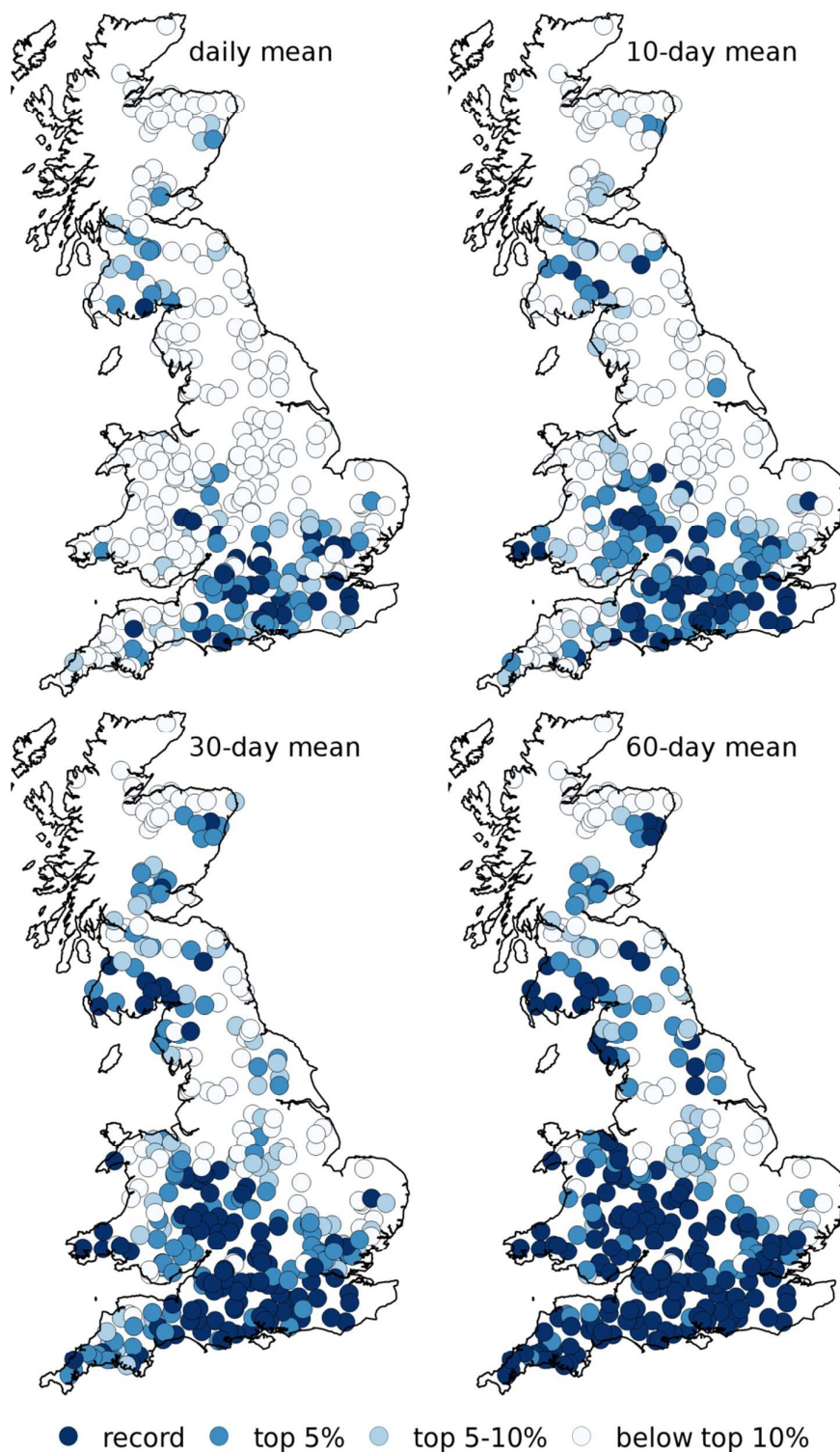


Figure 1 Maps showing the ranks of the maximum observed flows over December 2013–February 2014, for 1-, 10-, 30- and 60-day mean flows, for 342 gauges with at least 40 years of available data up to 2014.

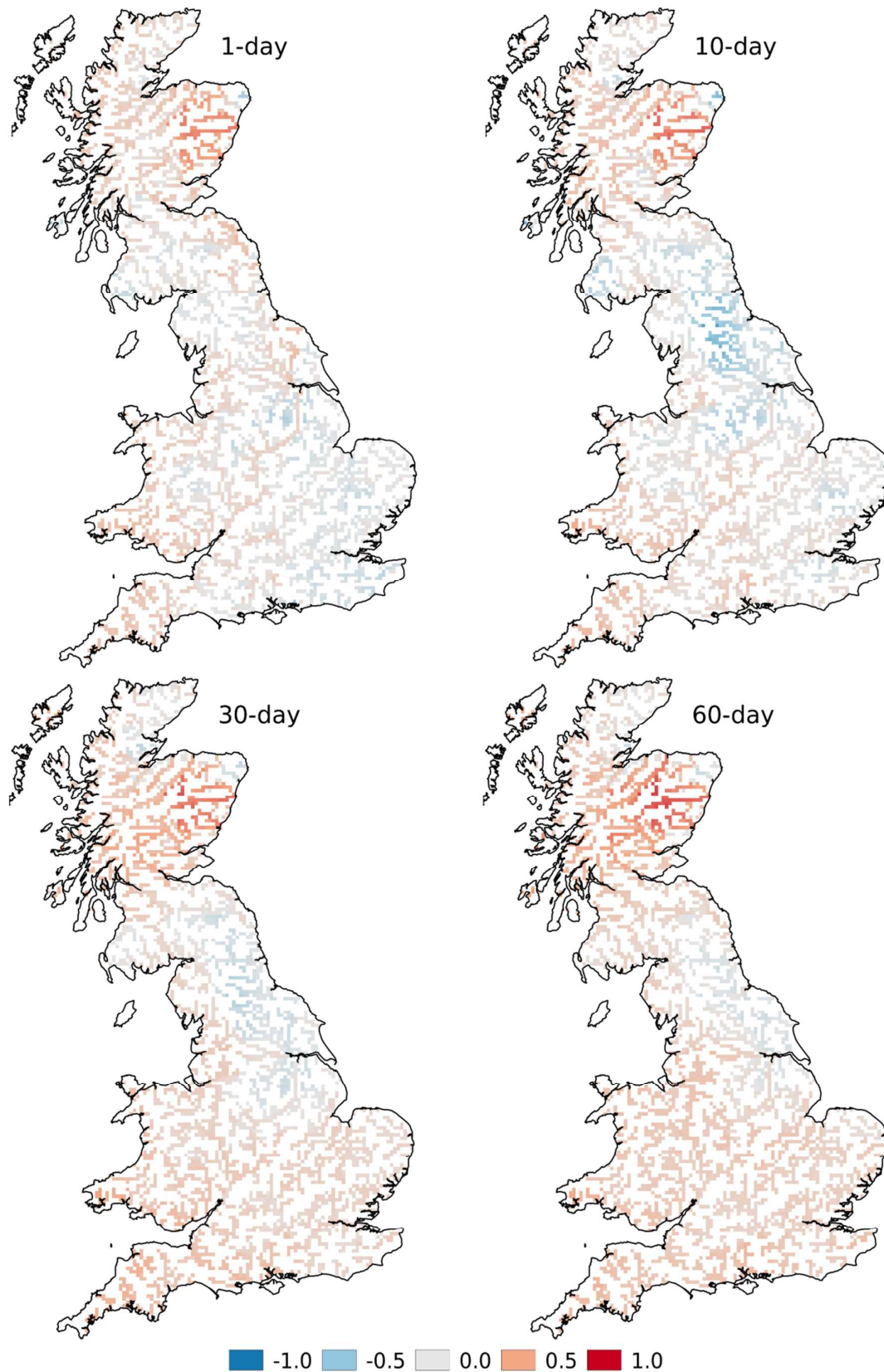


Figure 2 Maps of FAR values (using the pooled Natural ensemble), for 1-, 10-, 30- and 60-day mean flows.



Figure 3 a) Boxplots summarising the range of FAR values for eight regions across Britain (using the pooled Natural ensemble), for 1-, 10-, 30- and 60-day mean flows, when modelled with and without the snow modules. The boxes show the 25th-75th percentile range (with the black line showing the median), the whiskers show the 5th and 95th percentiles, and additional markers show minima and maxima. b) Region map.

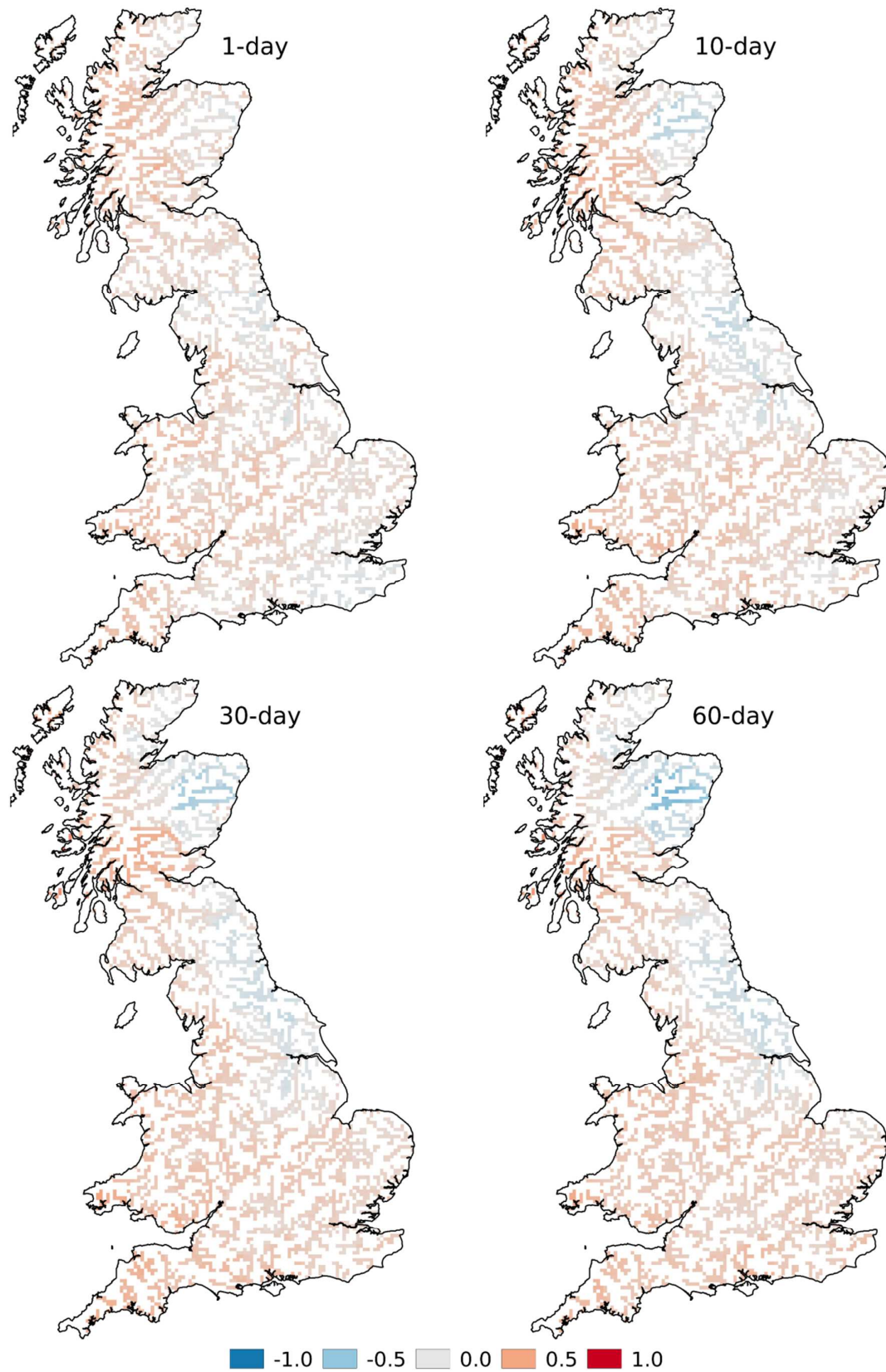


Figure 4 As Figure 2 but simulated without the snow module.

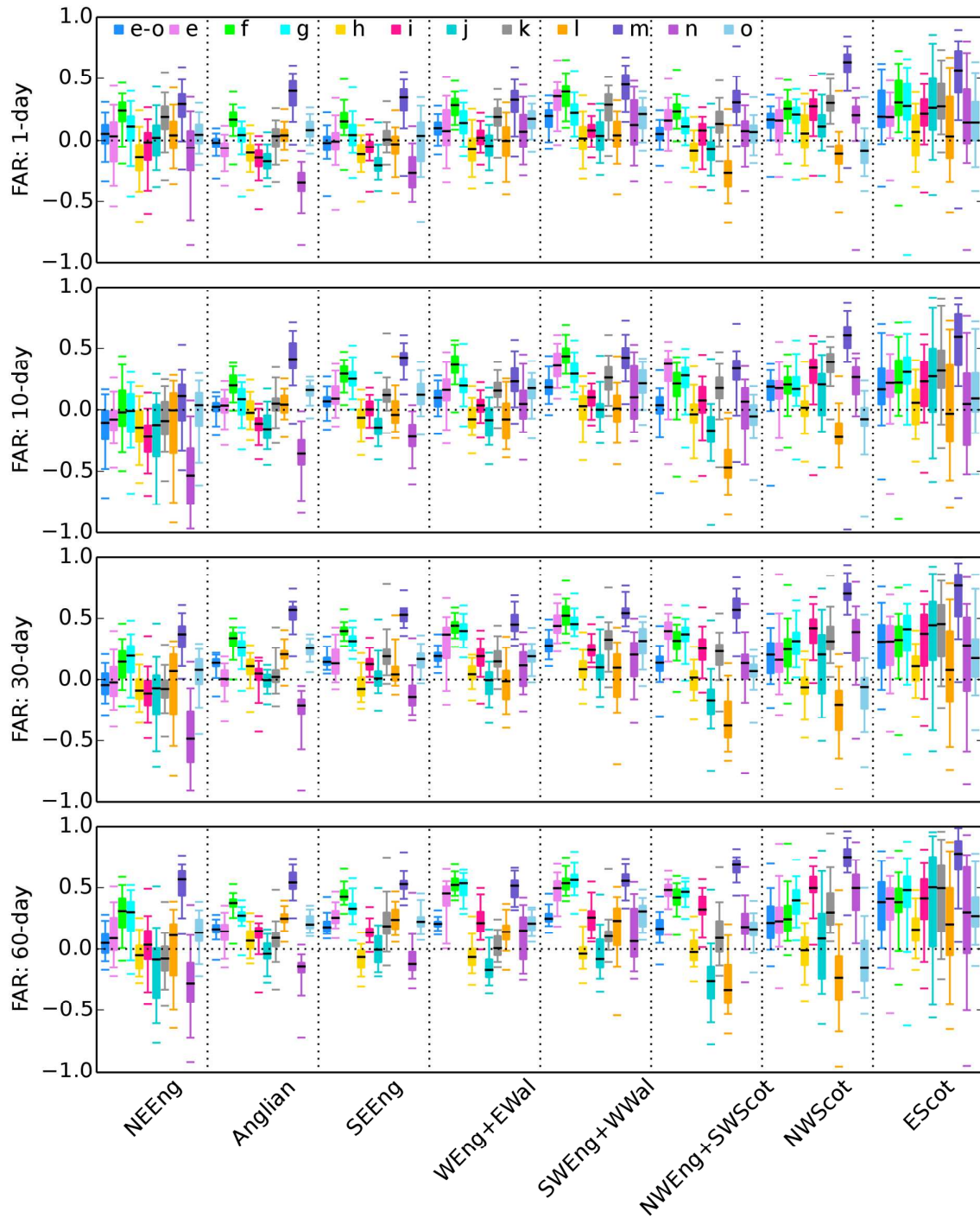


Figure 5 Boxplots summarising the range of FAR values for eight regions across Britain (Figure 3b) for 1-, 10-, 30- and 60-day mean flows, for the pooled Natural ensemble ('e-o') and each Natural ensemble ('e' to 'o') separately (see key). The boxes are defined as in Figure 3a.

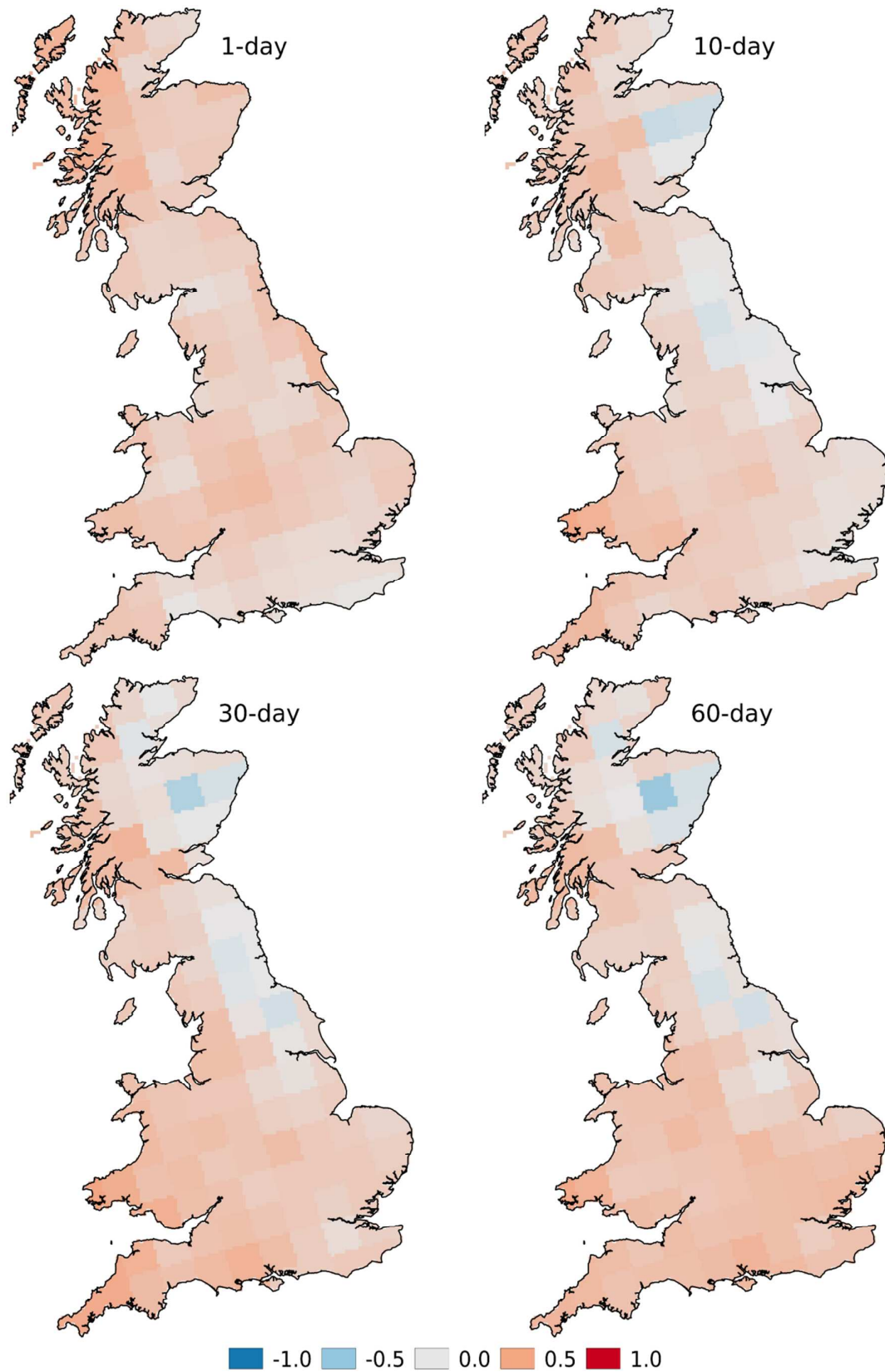


Figure 6 Maps of precipitation FAR values (using the pooled Natural ensemble), for 1-, 10-, 30- and 60-day accumulation periods.

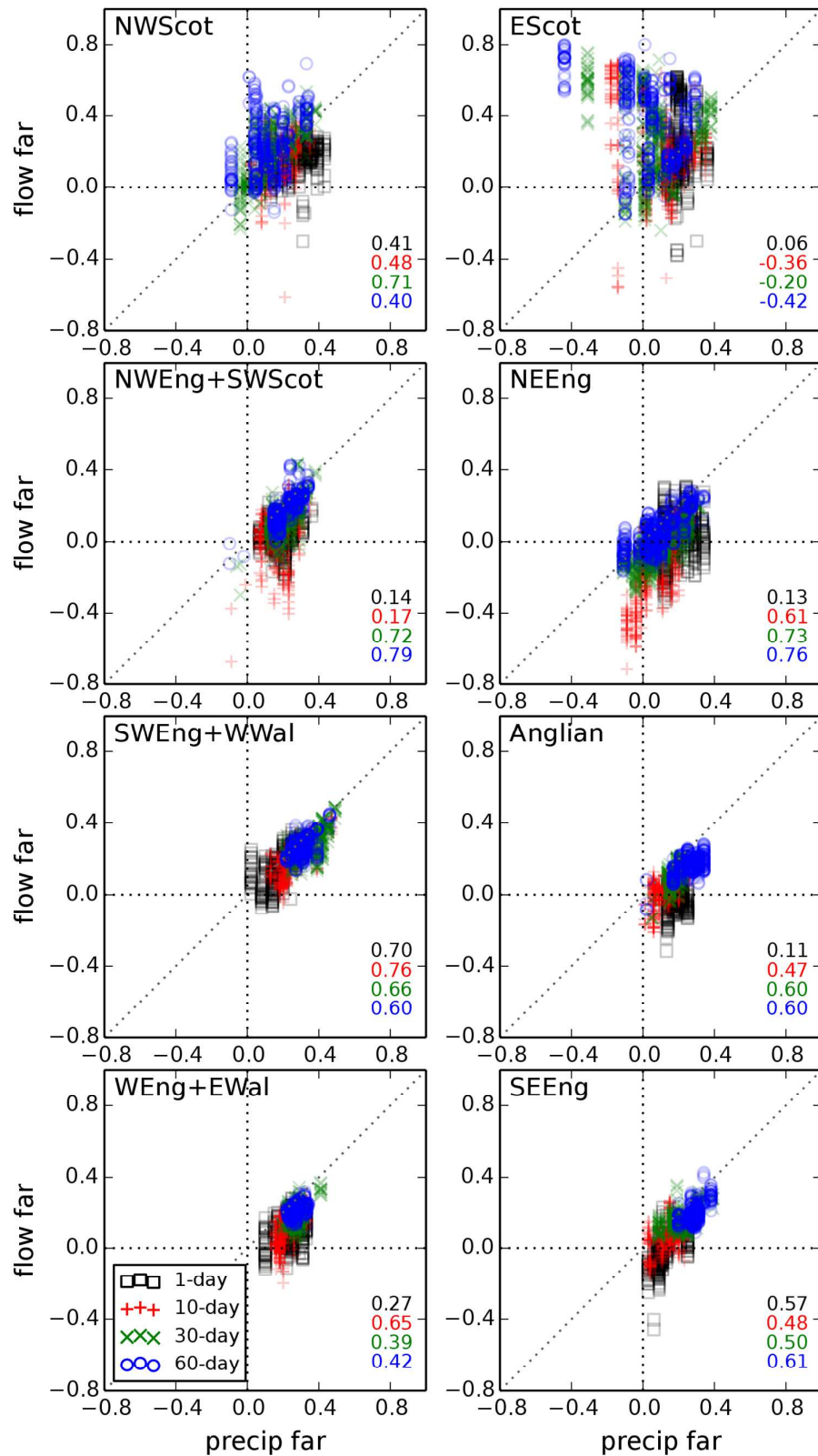


Figure 7 Scatter plots of flow FAR versus precipitation FAR (using the pooled Natural ensemble), for river points in eight regions across Britain (Figure 3b), for 1-, 10-, 30- and 60-day durations. The Pearson r correlation for each duration is shown in the bottom-right of each plot.

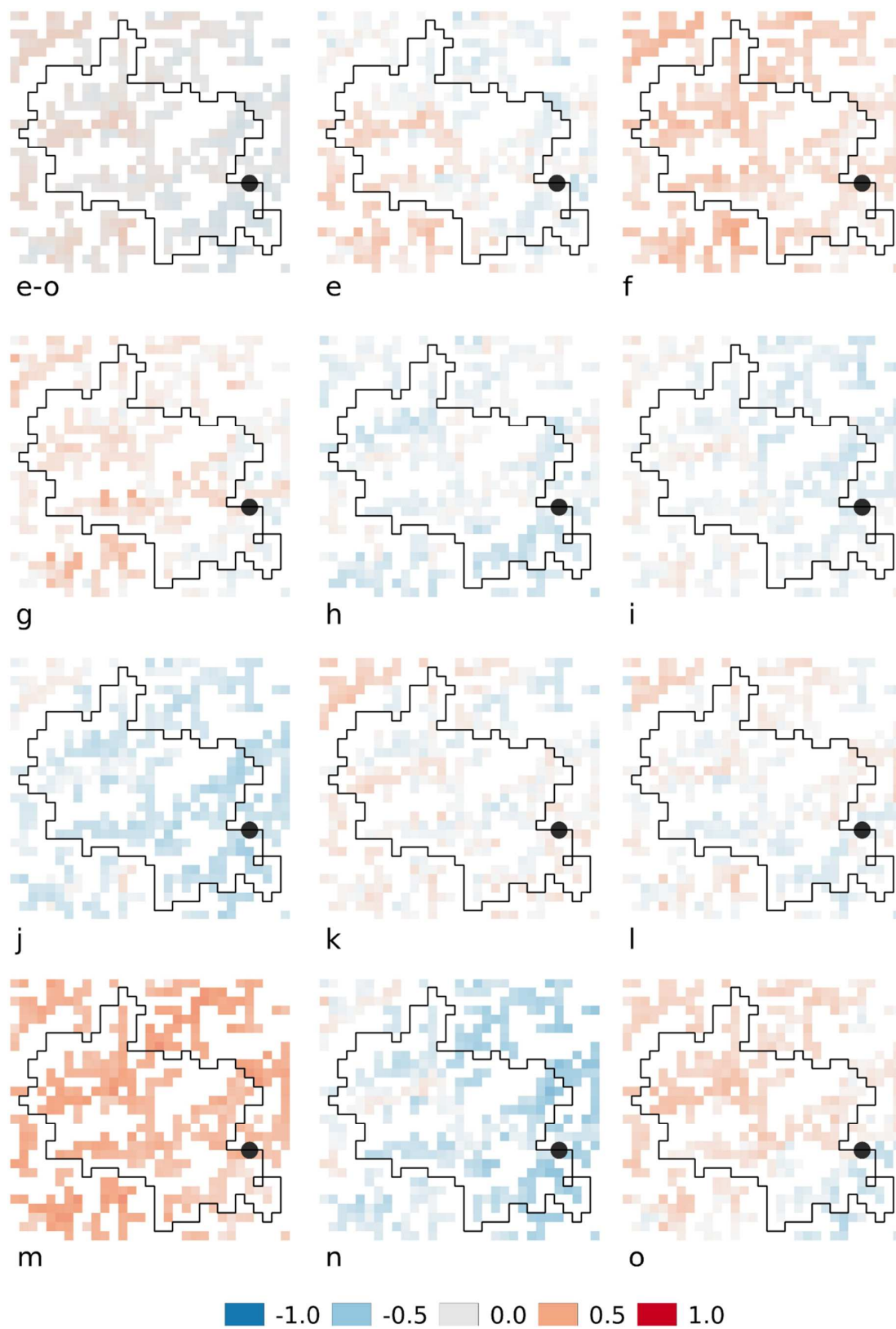


Figure 8 Maps of FAR values for 1-day mean flows in the Thames@Kingston catchment (black outline and dot), using the pooled Natural ensemble ('e-o') and each Natural ensemble ('e' to 'o') separately.

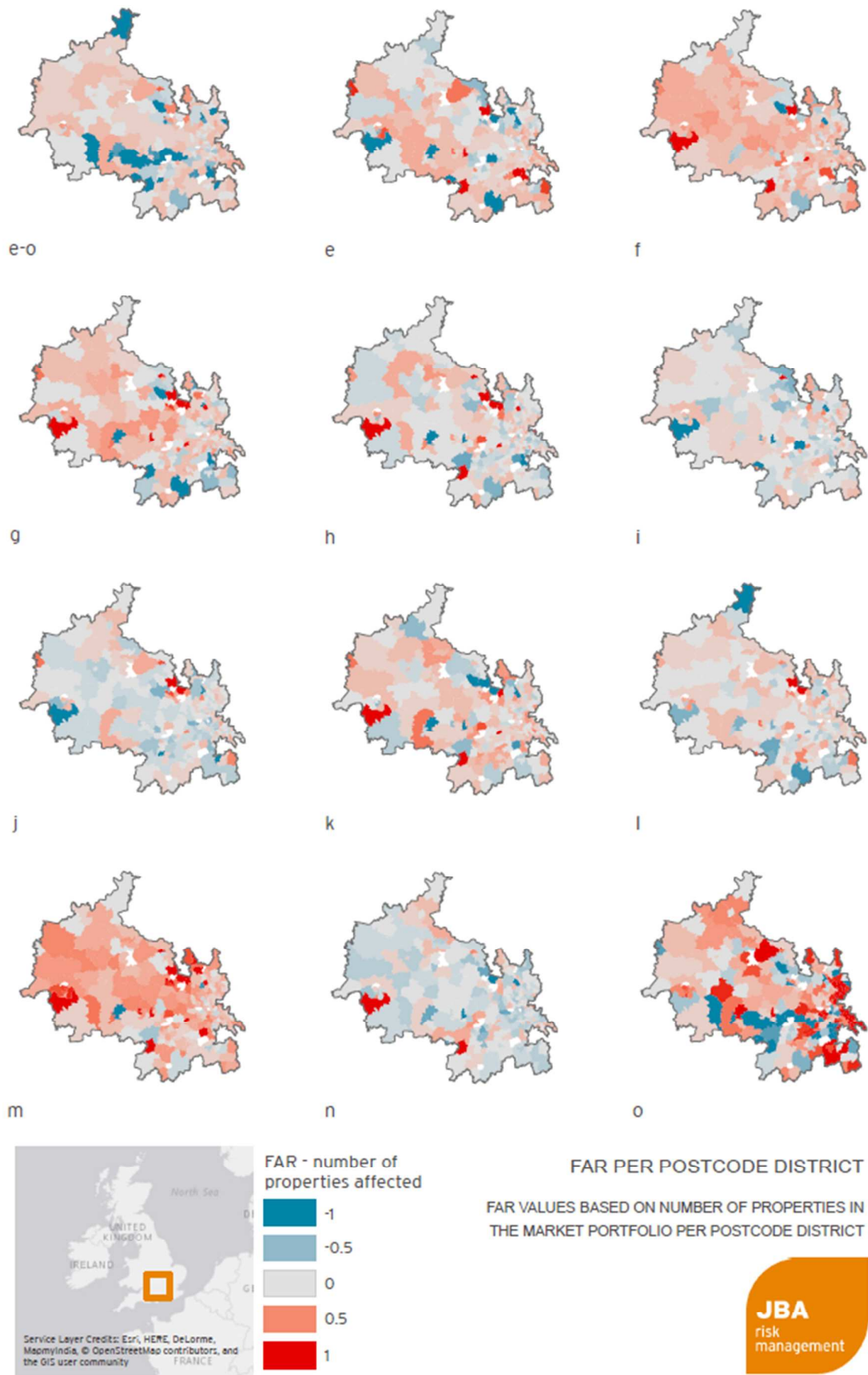


Figure 9 As Figure 8 but for flooded properties in each postcode district of the Thames@Kingston catchment.

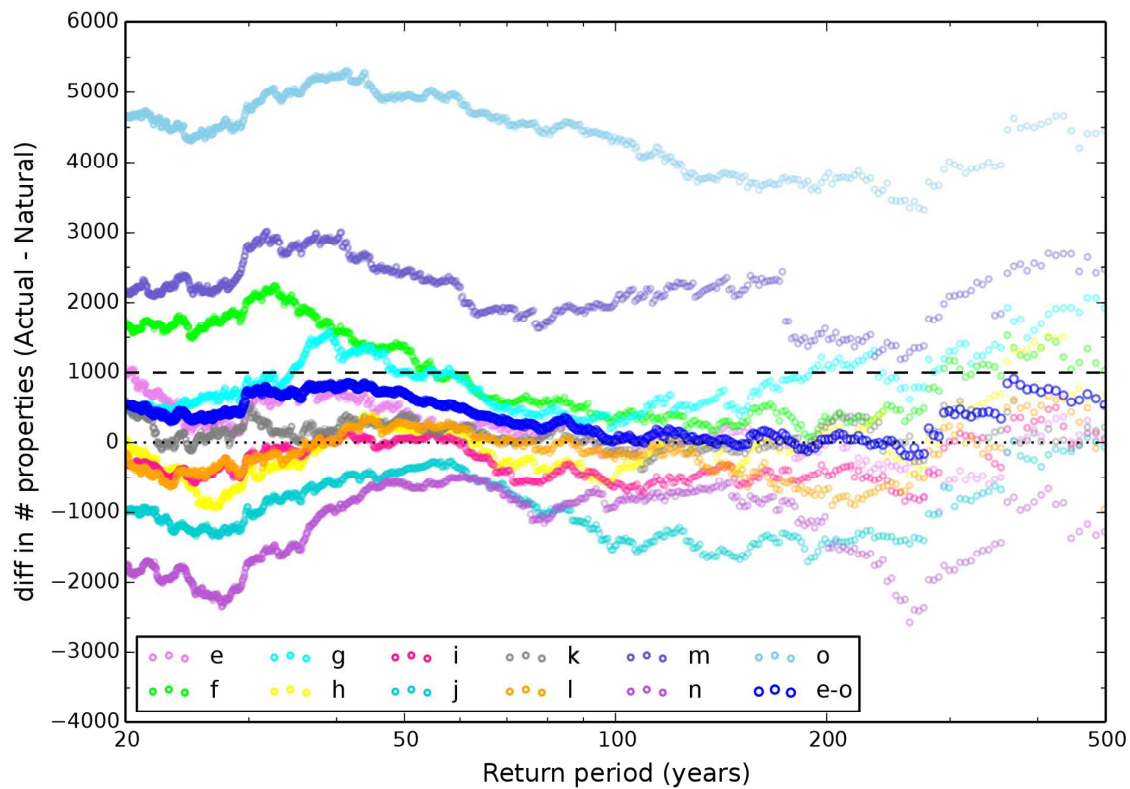
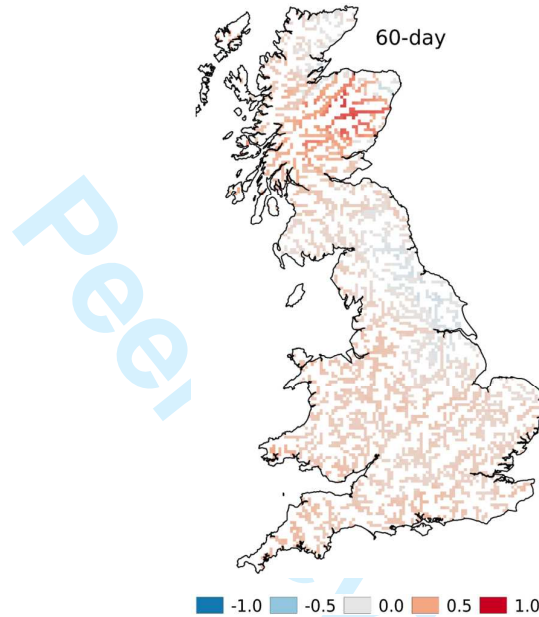


Figure 10 Difference between number of properties flooded in the Actual ensemble relative to the pooled Natural ensemble ('e-o') and each Natural ensemble ('e' to 'o') separately. Data are plotted as a function of relative level of extremeness within the ensemble (interpreted as a return period in years). The dashed line shows the estimate made by Schaller et al. (2016) under spatial uniformity assumptions.

Flood event attribution and damage estimation using national-scale grid-based modelling: Winter 2013/14

Kay A.L. *, Booth N., Lamb R., Raven E., Schaller N., Sparrow S.



The floods of Winter 2013/14 in Britain are assessed by combining ensembles of climate model data with a national-scale hydrological model. The results show that emissions are likely to have increased the chance of occurrence of these floods across much of the country (Fraction of Attributable Risk FAR > 0), with a stronger influence on longer duration peaks (FAR for peak 60-day mean flows shown in map above).